

A Variational Autoencoder for Heterogeneous Temporal and Longitudinal Data

Mine Öğretir, Siddharth Ramchandran, Dimitrios Papatheodorou, and Harri Lähdesmäki

Aalto University

Abstract. The variational autoencoder (VAE) is a popular deep latent variable model used to analyse high-dimensional datasets by learning a low-dimensional latent representation of the data. It simultaneously learns a generative model and an inference network to perform approximate posterior inference. Recently proposed extensions to VAEs that can handle temporal and longitudinal data have applications in healthcare, behavioural modelling, and predictive maintenance. However, these extensions do not account for heterogeneous data (i.e., data comprising of continuous and discrete attributes), which is common in many real-life applications. In this work, we propose the heterogeneous longitudinal VAE (HL-VAE) that extends the existing temporal and longitudinal VAEs to heterogeneous data. HL-VAE provides efficient inference for high-dimensional datasets and includes likelihood models for continuous, count, categorical, and ordinal data while accounting for missing observations. We demonstrate our model’s efficacy through simulated as well as clinical datasets, and show that our proposed model achieves competitive performance in missing value imputation and predictive accuracy.

Keywords: VAE, GP, Heterogeneous Data, Time-series

1 Introduction

Deep generative latent variable models are a popular choice of statistical models that are capable of learning complex data distributions, while simultaneously being an expressive unsupervised learning method. The ability of such models to efficiently learn the underlying data distribution in the presence of continuous latent variables was shown in the auto-encoding variational Bayes (AEVB) [7] technique. Building upon the idea of AEVB, the variational autoencoder (VAE) [7,23] model learns a low-dimensional latent distribution of the original dataset using a pair of deep neural networks.

The VAE model has become very popular across scientific disciplines, especially in modern biology, where VAEs have been used to analyse single-cell RNA sequencing [10] and microbiome data [16] as well as for protein modelling [6].

While the standard VAEs are proven to be powerful generative models for complex data modelling, they assume that the data samples are independent

of each other. To overcome this constraint, the i.i.d. standard Gaussian prior is replaced with a Gaussian process (GP) prior in recent work [2,3,19]. These GP prior VAEs can also utilise auxiliary covariates such as time, gender, and health condition. Thus, they can be used as conditional generative models.

Most of the variations of VAEs assume that the data is homogeneous, that is, all the data is assumed to be either continuous [7,19], binary [7], discrete [7,17,26], or in some other form, and the data is fully observed. However, in various real-world problems a dataset may have several different characteristics, such as ordinal, categorical, discrete/count data, and continuous data, which is called heterogeneous data. Furthermore, some of the information may be missing.

Temporal data refers to data samples collected over time, for example, laboratory measurements of a patient over a 5 year period. On the other hand, longitudinal data is a specific type of temporal data obtained from multiple, repeatedly measured subjects, and the data contains correlations among the observations within a single subject and across multiple subjects. For example, a clinical drug trial with several patients whose lab measurements are collected on several occasions over a 5 year period. Temporal and longitudinal studies are crucial in many fields, such as healthcare, economics, and social sciences, to name a few. In order for a VAE to be applicable to diverse real-life datasets, we require a model that: does not ignore the possible correlations between the latent embeddings across samples; does not assume that all the features in the data are modelled using the same type of distribution; and can handle missing observations while ensuring efficient computations. Some of the work on GP prior VAEs proposed approaches for modelling correlations between latent embeddings and handling missing observations [3,19], while Casale et al.[2] proposed a method to learn the auxiliary covariates from the data.

The longitudinal variational autoencoder (L-VAE) [19] is an extension of the VAE that is tailored to longitudinal data. It can model both time-varying shared as well as random effects through the use of a multi-output additive GP prior. However, the model makes the strong assumption that the observed data is normally distributed. On the other hand, the work by [15] proposed a general extension to the VAE that can handle both heterogeneous and missing data; however, it is not capable of longitudinal analysis. In this work, we build upon these ideas and propose a model that probabilistically encodes temporal and longitudinal measurements that may comprise of discrete as well as continuous (i.e., heterogeneous) data onto a low-dimensional homogeneous latent space while handling missing values that are missing completely at random (MCAR). The structured low-dimensional latent space dynamics are modelled using a multi-output additive GP prior as in [19], and the heterogeneous data can be reconstructed (or decoded) using a deep neural network based decoder.

The contributions of our work can be summarised as follows:

- We develop a VAE, the heterogeneous temporal and longitudinal variational autoencoder (HL-VAE), for heterogeneous time-series data that facilitates the modelling of the time-dependent dynamics with auxiliary covariate information and allows for a variety of observation likelihoods.

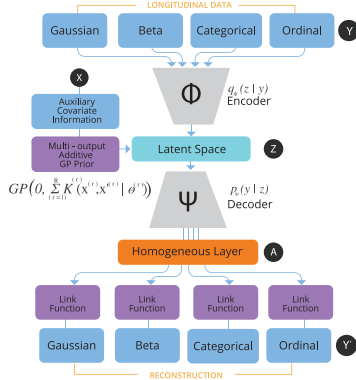


Fig. 1: HL-VAE overview.

- The heterogeneous model is incorporated into an efficient inference scheme so that large and high-dimensional data can be easily modelled.
- We compare our model’s performance against competing methods in missing value imputation as well as in long-term temporal and longitudinal prediction, and demonstrate the importance of assigning appropriate observation likelihoods in the heterogeneous data setting.

Our HL-VAE model is summarised in Fig. 1. The source code will be available upon publication.

2 Related work

VAEs The variational autoencoder [7,23] is a popular deep generative latent variable model that combines the strengths of amortised variational inference and graphical models in order to capture the low-dimensional latent structure of a high-dimensional, complex data distribution. However, VAEs assume that the latent representations are independent, and hence fails to capture the correlations between the data samples [7].

Gaussian process A Gaussian process (GP) is a flexible probabilistic model that captures the covariances between the samples and is commonly used in regression as well as classification tasks [21,22]. GPs have become popular machine learning methods especially in modelling time-series data [22,24]. Gaussian process latent variable model (GPLVM) is a GP variant that is specifically designed for embedding high-dimensional data points into a low-dimensional space [8]. Covariate GPLVM can utilise auxiliary covariates in adjusting the embedding [13].

Table 1: Comparison of related methods.

Models	Longitudinal study designs	Auxiliary covariates	Heterogeneous datasets	Minibatching	Reference
VAE	✗	✗	✗	✓	[7]
GPPVAE	✗	Limited	✗	Pseudo	[2]
GP-VAE	✗	✗	✗	✓	[4]
HI-VAE	✗	✗	✓	✓	[15]
L-VAE	✓	✓	✗	✓	[19]
HL-VAE	✓	✓	✓	✓	Our work

Models for heterogeneous data Various probabilistic models have been developed to handle data that comprises of both continuous and discrete features. Ramchandran et al. [18] extended the GPLVM to handle multiple likelihoods with a sampling-based variational inference technique. Their work enables heterogeneous datasets to be represented with low dimensional embeddings. Valera et al. [25] proposed a general Bayesian non-parametric latent variable model for heterogeneous datasets. Several authors ([1,15,11]) have introduced VAE-based methods for handling heterogeneous and incomplete data with various likelihood models. Nazabel et al. [15] proposed a model that enables the sharing of network parameters among different attributes for a single sample. Antelmi et al. [1] proposed a multi-channel approach, where each channel (each with a different likelihood) shares a common target prior on the latent representation. Ma et al. [11] trained individual marginal VAEs for every single variable to obtain the latent encoding for each variable and then fed them to a new multi-dimensional VAE. However, these models cannot capture any correlations among different samples. Although the models mentioned so far have not been designed for time-series or longitudinal datasets, methods that explore the domain of time-series data include, for example, the work of [14] that extends multi-output regression model for heterogeneous data. The approach by Gootjes et al. [5] enables longitudinal data modelling for heterogeneous datasets. They proposed a modular Bayesian network over the latent presentations of grouped variables obtained from HI-VAE so that each group of variables can be heterogeneous. However, their model requires a careful design of possible graph structures.

GP prior VAEs Various works have introduced GPs to VAEs in order to overcome the i.i.d. assumption of the latent representations of VAEs. Casale et al. [2] assumed a GP prior for the latent space of the VAE in order to incorporate the view and object information of the subjects. The GPPVAE model that they proposed assumes that the data is homogeneous (normally distributed). Moreover, its ability to model the subject-specific temporal structure is limited by the restrictive nature of the view-object GP product kernel. Fortuin et al. [4] proposed the GP-VAE model that assumes an independent GP prior on each subject’s time series. The model cannot capture temporal correlations across different subjects, and it does not utilise the auxiliary covariate information other than time. Ramchandran et al. [19] proposed the L-VAE, which is a VAE-based

model with a multi-output additive GP prior. L-VAE captures the structure of the low-dimensional embedding while utilising the auxiliary covariate information. They also proposed an efficient minibatch-based GP inference scheme. Even though L-VAE has a comprehensive capability to capture shared temporal structure as well as individual temporal structure with the help of auxiliary covariates, it assumes that the data is normally distributed, which is a major shortcoming in the modelling of longitudinal data. Our model addresses these shortcomings while capturing the correlations among individual subjects and temporal dependencies. We handle the various challenges of incorporating heterogeneous data while effectively building on the benefits offered by GPs and VAEs. Table 1 compares our method with the prime related methods.

3 Background

Notation: In our setting, the data consists of samples, \mathbf{y}_i , and their covariate information, \mathbf{x}_i . The domain of \mathbf{x}_i is $\mathcal{X} = \mathcal{X}_1 \times \dots \times \mathcal{X}_Q$, where Q is the number of auxiliary covariates and \mathcal{X}_q is the domain of the q^{th} covariate which can be continuous, categorical, or binary. The domain of \mathbf{y}_i is $\mathcal{Y} = \mathcal{Y}_1 \times \dots \times \mathcal{Y}_D$, where D is the dimensionality of the observed data. We assume that the variables of \mathbf{y} are heterogeneous and that each \mathcal{Y}_d can define a numerical domain (real, positive real, count, etc.) or a nominal domain (categorical or ordinal). We will define the heterogeneous domains in detail in Section 4.

A temporal dataset of size N is represented with $X = [\mathbf{x}_1, \dots, \mathbf{x}_N]^T$ and $Y = [\mathbf{y}_1, \dots, \mathbf{y}_N]^T$, where N is the number of samples taken over time for an instance (e.g. an individual patient). For a longitudinal dataset, let P denote the number of unique instances (e.g. individuals, patients, etc.), and n_p denote the number of time-series samples from instance p . Therefore, the total number of longitudinal samples is $N = \sum_{p=1}^P n_p$. A pair $X_p = [\mathbf{x}_1^p, \dots, \mathbf{x}_{n_p}^p]^T$ and $Y_p = [\mathbf{y}_1^p, \dots, \mathbf{y}_{n_p}^p]^T$ represents the time-series data for an individual p , where $\mathbf{x}_t^p \in \mathcal{X}$ and $\mathbf{y}_t^p \in \mathcal{Y}$ denotes the auxiliary covariate information and dependent variables, respectively. We denote longitudinal data as (X, Y) , where $X = [X_1^T, \dots, X_P^T]^T = [\mathbf{x}_1, \dots, \mathbf{x}_N]^T$ and $Y = [Y_1^T, \dots, Y_P^T]^T = [\mathbf{y}_1, \dots, \mathbf{y}_N]^T$. The low-dimensional latent embedding of Y is denoted as $Z = [\mathbf{z}_1, \dots, \mathbf{z}_N]^T = [\bar{\mathbf{z}}_1, \dots, \bar{\mathbf{z}}_L] \in \mathbb{R}^{N \times L}$. For example, in a clinical healthcare dataset X would represent the patient-specific information such as the patient identifier, age, height, weight, sex, etc. and Y would represent the various lab measurements.

3.1 VAE for Heterogeneous Data

In standard VAE models, the generative likelihood of the observed data is modelled as normally distributed. However in real-life applications, such as in healthcare, the data is typically heterogeneous. In order to effectively capture the different data characteristics, the generative model should be able to handle different likelihood distributions. Nazabal et al. [15] suggested a VAE model (HI-VAE) that can handle different likelihood parameters and, at the same time, capture

the statistical dependencies among the differently distributed data dimensions. The generative model for the n^{th} heterogeneous data point is

$$p_{\omega}(\mathbf{y}_n, \mathbf{z}_n) = p_{\theta}(\mathbf{z}_n) \prod_{d=1}^D p_{\psi}(y_{nd} \mid \gamma_{nd}) \quad (1)$$

$$\gamma_{nd} = \mathbf{h}_d(\mathbf{a}_{nd}) \quad \mathbf{A}_n = [\mathbf{a}_{n1}, \dots, \mathbf{a}_{nD}] = \mathbf{g}(\mathbf{z}_n),$$

where γ_{nd} represents the likelihood parameters of the d^{th} dimension that are obtained from independent neural networks $\mathbf{h}_d(\cdot)$, $d \in \{1, \dots, D\}$ and $\mathbf{A}_n \in \mathbb{R}^S$ is a so-called homogeneous layer where $S = s_1 + \dots + s_D$ denotes the total number of dimension for each independent neural network, i.e., $s_d = |\mathbf{a}_{nd}|$.

We can approximate the true posterior with a variational posterior as in the standard VAE: $q_{\phi}(\mathbf{z}_n \mid \mathbf{y}_n) = \mathcal{N}(\boldsymbol{\mu}_{\phi}(\tilde{\mathbf{y}}_n), \boldsymbol{\Sigma}_{\phi}(\tilde{\mathbf{y}}_n))$, where $\boldsymbol{\mu}_{\phi}$ and $\boldsymbol{\Sigma}_{\phi}$ are the encoder networks, and $\tilde{\mathbf{y}}$ represents the encoder input with missing values replaced by zeros. In order to handle missing data in X , the ELBO is computed only over the observed data. With the generative model in Eq. 1, the likelihoods of the data can be modelled with various distributions.

3.2 Gaussian Process Prior VAE

The standard VAE model assumes that the joint distribution factorises across the samples. On the other hand, GPs are well-suited to model these correlations. Extension of VAEs, such as GPPVAE [2], GP-VAE [3] and L-VAE [19], combine VAEs with GPs. These methods use a GP prior (instead of a standard Gaussian prior) in the latent space of a VAE to model multivariate temporal and longitudinal data.

The standard VAE assumes a factorisable prior on the latent space $p_{\theta}(Z) = \prod_{i=1}^N p_{\theta}(\mathbf{z}_i)$, and does not utilise the covariate information of the data. Meanwhile, the prior for the latent variables of the GP prior VAEs $p_{\theta}(Z \mid X)$ corresponds to a GP prior which factorises across the latent dimensions. Specifically, for each of the $l \in \{1, \dots, L\}$ dimensions, the latent model is $f_l(\mathbf{x}) \sim \mathcal{GP}(\mu_l(\mathbf{x}), k_l(\mathbf{x}, \mathbf{x}'))$, where $\mu_l(\mathbf{x})$ and $k_l(\mathbf{x}, \mathbf{x}')$ are the mean and the covariance function (CF) of any pair of auxiliary covariates \mathbf{x} and \mathbf{x}' . We assume the mean as 0. Consequently, the GP prior can be written as

$$p_{\theta}(Z \mid X) = \prod_{l=1}^L p_{\theta}(\bar{\mathbf{z}}_l \mid X) = \prod_{l=1}^L \mathcal{N}(\bar{\mathbf{z}}_l \mid \mathbf{0}, \boldsymbol{\Sigma}_l + \sigma_l^2 I_N), \quad (2)$$

where $\boldsymbol{\Sigma}_l = K_{XX}^{(l)}$ is the $N \times N$ covariance matrix corresponding to the CF of the GP component of the l^{th} latent dimension: $k_l(\mathbf{x}, \mathbf{x}')$.

We formulate our method using the L-VAE model which assumes additive covariance functions. L-VAE proposes more general and flexible CFs than other methods (GPPVAE and GP-VAE), and the other methods can indeed be seen as special cases of the more general L-VAE model. The L-VAE model specifies the structure of the data among the observed samples Y with an additive

multi-output GP prior over the latent space whose CF depend on the auxiliary covariates X , as described in [19].

The generative model of L-VAE is formulated as:

$$p_\omega(Y | X) = \int_Z p_\psi(Y | Z, X) p_\theta(Z | X) dZ = \int_Z \prod_{n=1}^N p_\psi(y_n | z_n) p_\theta(Z | X) dZ, \quad (3)$$

where $\omega = \{\psi, \theta\}$ is the parameter set and the probabilistic decoder, $p_\psi(y_n | z_n)$, is assumed to be normally distributed. The prior for the latent variables, $p_\theta(Z | X)$, corresponds to the multi-output additive GP prior which factorises across the latent dimensions as in Eq. 2. Specifically, for each of the $l \in \{1, \dots, L\}$ dimensions the latent model is $f_l(\mathbf{x}) = f_l^{(1)}(\mathbf{x}^{(1)}) + \dots + f_l^{(R)}(\mathbf{x}^{(R)})$ where $f_l^{(r)}(\mathbf{x}^{(r)}) \sim \mathcal{GP}(\mathbf{0}, k_l^{(r)}(\mathbf{x}^{(r)}, \mathbf{x}^{(r)\prime}))$, R refers to the total number of additive components, and each separate GP, $f_l^{(r)}(\mathbf{x}^{(r)})$, depends only on a small subset of covariates $\mathbf{x}^{(r)} \in \mathcal{X}^{(r)} \subset \mathcal{X}$. The covariance matrix of the GP prior in Eq. 2 leads to $\Sigma_l = \sum_{r=1}^R K_{XX}^{(r,l)}$, where $K_{XX}^{(r,l)}$ is the $N \times N$ covariance matrix corresponding to the CF of the r^{th} GP component of the l^{th} latent dimension: $k_l^{(r)}(\mathbf{x}^{(r)}, \mathbf{x}^{(r)\prime})$.

The variational posterior of Z to approximate the true posterior is defined as the product of multivariate Gaussian distributions across samples, $q_\phi(Z | Y) = \prod_{n=1}^N \prod_{l=1}^L \mathcal{N}(z_{nl} | \mu_{\phi,l}(\tilde{\mathbf{y}}_n), \sigma_{\phi,l}^2(\tilde{\mathbf{y}}_n))$ where the probabilistic encoder is represented by neural network functions $\mu_{\phi,l}$ and $\sigma_{\phi,l}^2$ (parameterised by ϕ) that determines the means as well as the variances of the approximating variational distribution. The ELBO for L-VAE as derived in [19], is as follows:

$$\begin{aligned} \log p_\omega(Y | X) &\geq \mathcal{L}(\phi, \psi, \theta; Y, X) \\ &\triangleq \mathbb{E}_{q_\phi(Z|Y)} [\log p_\psi(Y | Z)] - D_{\text{KL}}(q_\phi(Z | Y) || p_\theta(Z | X)). \end{aligned} \quad (4)$$

The first term in Eq. 4 is the reconstruction loss, which does not involve the GP and can be obtained directly as

$$\mathbb{E}_{q_\phi(Z|Y)} [\log p_\psi(Y | Z)] = \sum_{n=1}^N \sum_{d=1}^D \mathbb{E}_{q_\phi(z_n | \mathbf{y}_n)} [\log p_\psi(y_{nd} | z_n)]. \quad (5)$$

The second term is the KL divergence between the variational posterior of Z and the multi-output additive GP prior over the latent variables, $D_{\text{KL}} \triangleq D_{\text{KL}}(q_\phi(Z | Y) || p_\theta(Z | X))$, which also factorises across the L latent dimensions: $D_{\text{KL}} = \prod_{l=1}^L D_{\text{KL}}(q_\phi(\bar{z}_l | Y, X) || p_\theta(\bar{z}_l | X))$. Each of the KL divergences are available in closed-form. However, its exact computation takes $\mathcal{O}(N^3)$.

Ramchandran et al. [19] proposed a mini-batch compatible upper bound for this KL divergence that scales linearly to big data. Briefly, the method separates the individual specific random component (i.e., additive GP component that corresponds to the interaction between instances and time) from the other additive components of the covariance function. Therefore (and ignoring the subscript l for clarity), the covariance matrix can be written as

$\Sigma = K_{XX}^{(A)} + \hat{\Sigma}$, where $K_{XX}^{(A)} = \sum_{r=1}^{R-1} K_{XX}^{(r)}$ contains the first $R-1$ components, and does not have an interaction between instances and time. The last term contains the individual-specific random component $\hat{\Sigma} = \text{diag}(\hat{\Sigma}_1, \dots, \hat{\Sigma}_P)$, where $\hat{\Sigma}_p = K_{X_p X_p}^{(R)} + \sigma_z^2 I_{n_p}$. The efficient KL upper bound is then obtained by assuming the standard low-rank inducing point approximation for $K_{XX}^{(A)}$ with M inducing points $S = (s_1, \dots, s_M)$, and the corresponding outputs $\mathbf{u} = (f(s_1), \dots, f(s_M))^T = (u_1, \dots, u_M)^T$ (separately for each latent dimension l):

$$\hat{D}_{\text{KL}} \leq \frac{1}{2} \frac{P}{\hat{P}} \sum_{p \in \mathcal{P}} \Upsilon_p - \frac{N}{2} + D_{\text{KL}}(\mathcal{N}(\mathbf{m}, H) \parallel \mathcal{N}(\mathbf{0}, K_{SS}^{(A)})), \quad (6)$$

where the summation is over a subset of unique instances $\mathcal{P} \subset \{1, \dots, P\}$ with $|\mathcal{P}| = \hat{P}$, Υ_p involves computing a quantity for instance p (see [19]), and \mathbf{m} and H are the global variational parameters for $\mathbf{u} \sim \mathcal{N}(\mathbf{m}, H)$. For a detailed derivation, we refer the reader to [19].

4 Heterogeneous Temporal and Longitudinal VAE

In this work, we extend the GP prior VAE models to handle heterogeneous data that may contain missing values. The generative model of our HL-VAE is formulated as in Eq. 3, but makes use of a heterogeneous likelihood:

$$p_{\omega}(Y \mid X) = \int_Z \underbrace{p_{\psi}(Y \mid Z, X)}_{\text{Heterogeneous likelihood}} \underbrace{p_{\theta}(Z \mid X)}_{\text{GP prior}} dZ,$$

where $\omega = \{\psi, \theta\}$ is the set of parameters, and the data is modelled with a heterogeneous likelihood:

$$p_{\psi}(Y \mid Z, X) = \prod_{n=1}^N p_{\psi}(\mathbf{y}_n \mid \mathbf{z}_n) = \prod_{n=1}^N \prod_{d=1}^D p_{\psi}(y_{nd} \mid \gamma_{nd}) \quad (7)$$

$$\gamma_{nd} = [l_1(\mathbf{h}_{1d}(\mathbf{a}_{nd})), \dots, l_W(\mathbf{h}_{Wd}(\mathbf{a}_{nd}))] \quad (8)$$

$$\mathbf{A}_n = [\mathbf{a}_{n1}, \dots, \mathbf{a}_{nD}] = \mathbf{g}_{\psi}(\mathbf{z}_n). \quad (9)$$

The decoder \mathbf{g}_{ψ} first maps the latent code of the n^{th} sample, \mathbf{z}_n , to a homogeneous array (or layer) of outputs $\mathbf{A}_n \in \mathbb{R}^{U \times D}$, where U is the user-chosen depth (Eq. 9). The d^{th} column of the layer, \mathbf{a}_{nd} , is then passed through W independent neural networks \mathbf{h}_{wd} (Eq. 8) where W is the number of likelihood parameters for the d^{th} feature and the networks \mathbf{h}_{wd} have parameters that are optimised. Finally, outputs of the neural networks $\mathbf{h}_{1d}, \dots, \mathbf{h}_{Wd}$ are passed through link functions l_1, \dots, l_W that define the likelihood parameters γ_{nd} for the d^{th} feature $y_{nd} \in \mathcal{Y}_d$ with a specific likelihood model (Eq. 8). We define the link functions for a variety of likelihood models below, and our model can be easily extended to other likelihoods as well.

Gaussian distribution: For the Gaussian likelihood, the likelihood parameters are given as $\gamma_{nd} = \{l_1(\mathbf{h}_{1d}(\mathbf{a}_{nd})), l_2(\mathbf{h}_{2d}(\mathbf{a}_{nd}))\}$, where the parameters correspond to the mean and the variance respectively, and $W = 2$. The link functions, $l_1(\cdot)$ and $l_2(\cdot)$, constrain the mean and the variance of the likelihood. If the data is within the interval $[0, 1]$, we make use of the *sigmoid* function for $l_1(\cdot)$. In all other cases, we choose $l_1(\cdot)$ to be the identity function. The variance is constrained to be positive by choosing the *softplus* function for $l_2(\cdot)$. Likelihood parameters can also be modelled as $\gamma_{nd} = \{l_1(\mathbf{h}_{1d}(\mathbf{a}_{nd})), l_2(\sigma_d)\}$ with a learnable free-variance parameter across the dataset for each variable.

Log-normal distribution: For the log-normal distribution, the logarithm of the data is said to be normally distributed. The likelihood parameters, γ_{nd} , are similar to the Gaussian distribution. Moreover, we make use of the identity function for $l_1(\cdot)$ and *softplus* function for $l_2(\cdot)$.

Beta distribution: We assume a re-parameterised distribution for the beta likelihood. The distribution is parameterised by the mean and the inverse dispersion parameter which is a shared parameter that is optimised. The likelihood parameters are given as $\gamma_{nd} = \{l_1(\mathbf{h}_{1d}(\mathbf{a}_{nd}))l_2(\nu_d), (1 - l_1(\mathbf{h}_{1d}(\mathbf{a}_{nd})))l_2(\nu_d)\}$. We choose $l_1(\cdot)$ to be the CDF of the standard normal distribution and $l_2(\cdot)$ to be the *softplus* function. Note that the role of $l_2(\cdot)$ is to constrain the inverse dispersion parameter (ν_d) to be positive.

Poisson distribution: The Poisson likelihood is specified by a single positive parameter (the rate parameter). The likelihood parameters are given as $\gamma_{nd} = \{l_1(\mathbf{h}_{1d}(\mathbf{a}_{nd}))\}$ and $W = 1$. We make use of the *softplus* function for $l_1(\cdot)$ in order to constrain the parameter to non-negative values.

Categorical distribution: For the categorical likelihood, the data with R categories is represented using one-hot encoding and we utilise a multinomial logit model. We make use of the output of a neural network to represent the unnormalised probabilities for $R - 1$ categories (i.e. except the first category). The log-probability of the first category is set to 0. Therefore, the probability of each category r is: $p_\psi(y_{nd} = r | \gamma_{nd}) = \frac{\exp(-\mathbf{h}_{rd}(\mathbf{a}_{nd}))}{\sum_{q=1}^R \exp(-\mathbf{h}_{qd}(\mathbf{a}_{nd}))}$, where $\gamma_{nd} = \{0, l_1(\mathbf{h}_{1d}(\mathbf{a}_{nd})), \dots, l_{R-1}(\mathbf{h}_{R-1d}(\mathbf{a}_{nd}))\}$ and all the link functions are identity functions.

Ordinal distribution: Assuming R levels, we represent the ordinal data with the thermometer encoding and make use of the ordinal logit model. The probability for each level is computed as $p_\psi(y_{nd} = r | \gamma_{nd}) = p(y_{nd} \leq r | \gamma_{nd}) - p(y_{nd} \leq r - 1 | \gamma_{nd})$ where $p(y_{nd} \leq r | \gamma_{nd}) = \frac{1}{1 + \exp(-(l_r(\theta_r) - c_d(\mathbf{a}_{nd})))}$, $\gamma_{nd} = \{c_d(\mathbf{a}_{nd}) = l_1(h_{1d}(\mathbf{a}_{nd})), l_2(\theta_1), \dots, l_2(\theta_{R-1})\}$, and $W = 1$. We choose the *softplus* function as the link functions. The threshold values $\theta_1, \dots, \theta_{R-1}$ are modelled as free parameters.

Approximating the true posterior with a variational posterior, the ELBO has the same form as in Eq. 4 except that the

$$\mathbb{E}_{q_\phi(Z|Y)}[\log p_\psi(Y | Z)] = \sum_{n=1}^N \sum_{d \in O_n} \mathbb{E}_{q_\phi(\mathbf{z}_n | \mathbf{y}_n^o)} [\log p_\psi(y_{nd} | \gamma_{nd})]. \quad (10)$$

In Eq. 10, O_n corresponds to the index set of the observed variables of \mathbf{y}_n , and \mathbf{y}_n^o represents the observed part of \mathbf{y}_n (i.e. a slice of \mathbf{y}_n that only contains the elements index by O_n). The KL divergence is computed as in the case of exact inference or as in Eq. 6 (in case of mini-batch compatible SGD).

4.1 Predictive distribution

The trained model with parameters ϕ, ψ, θ can be used for making future predictions given the beginning of a sequence as well as for imputing the missing values for a given data sample. Using the learned variational approximation $q_\phi(Z | Y, X)$ in place of the intractable true posterior $p_\omega(Z | Y, X)$, the predictive distribution can be written as

$$\begin{aligned} p_\omega(\mathbf{y}_* | \mathbf{x}_*, Y, X) &\approx \int_{\mathbf{z}_*, Z} p_\psi(\mathbf{y}_* | \mathbf{z}_*) p_\theta(\mathbf{z}_* | \mathbf{x}_*, Z, X) q_\phi(Z | Y, X) d\mathbf{z}_* dZ \\ &= \int_{\mathbf{z}_*} \prod_{d=1}^D p_\psi(y_{*d} | \gamma_{*d}) \prod_{l=1}^L \mathcal{N}(z_{*l} | \mu_{*l}, \sigma_{*l}^2) d\mathbf{z}_*, \end{aligned}$$

where \mathbf{y}_* , \mathbf{x}_* , and \mathbf{z}_* are the unseen test data, its associated covariates, and its corresponding latent embeddings respectively. As stated in [19], the means of the latent embeddings are $\mu_{*l} = K_{\mathbf{x}_* X}^{(l)} \Sigma_l^{-1} \bar{\mu}_l$ and its variances are $\sigma_{*l}^2 = k_l(\mathbf{x}_*, \mathbf{x}_*) - K_{\mathbf{x}_* X}^{(l)} \Sigma_l^{-1} K_{X \mathbf{x}_*}^{(l)} + K_{\mathbf{x}_* X}^{(l)} \Sigma_l^{-1} W_l \Sigma_l^{-1} K_{X \mathbf{x}_*}^{(l)} + \sigma_{z_l}^2$, where $\bar{\mu}_l$ and W_l contain the encoded means and variances for all the N training data points, and $\Sigma_l = \sum_{r=1}^R K_{XX}^{(l,r)} + \sigma_{z_l}^2 I_N$.

5 Experiments

The ability of our model to effectively learn the underlying heterogeneous data distribution is evaluated through the model's performance in imputing missing values in the training data as well as in the unseen test data, and through the model's ability in predicting future observations. We demonstrate the efficacy of our model on two modified MNIST datasets to simulate temporal and longitudinal datasets as well as on a real clinical dataset from the Parkinson's Progression Markers Initiative (PPMI). We compare our model's performance against the Heterogeneous Incomplete Variational Autoencoder (HI-VAE) [15] and the Longitudinal Variational Autoencoder (L-VAE) [19]. HI-VAE is one of the state-of-the-art VAE-based models in heterogeneous data imputation. However, it does not have explicit support for longitudinal data. On the other hand, L-VAE has demonstrated its effectiveness to successfully model longitudinal data. However, L-VAE makes the strong assumption that the data is Gaussian distributed. Through our experiments, we demonstrate how an appropriate choice of likelihood distributions results in improved performance for temporal and longitudinal VAEs.

The additive components with different covariate functions (CF) for the additive multi-output GP prior are denoted as: $f_{se}(\cdot)$ for squared exponential CF,

$f_{\text{ca}}(\cdot)$ for categorical CF, and $f_{\text{ca} \times \text{se}}(\cdot \times \cdot)$ for their interaction. In all the experiments, we have ensured that the neural network structures are as comparable as possible. The details of the error metrics, more information on the PPMI dataset and the network structures can be found in the Supplementary Materials.

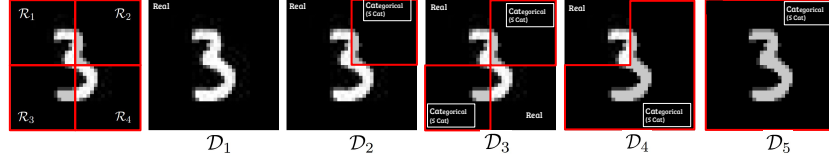


Fig. 2: Heterogeneous data configuration for temporal and longitudinal MNIST dataset. Each digit comprises of 4 regions $\mathcal{R}_1, \dots, \mathcal{R}_4$. Moreover, $\mathcal{R}_i \sim \mathcal{N}$ denotes Gaussian likelihood for pixels in region \mathcal{R}_i , and $\mathcal{C}_j \sim \mathcal{C}_5$ denotes categorical likelihood with 5 levels for pixels in region \mathcal{R}_j . The datasets are simulated as follows: $\mathcal{D}_1 = \{\mathcal{R}_1, \mathcal{R}_2, \mathcal{R}_3, \mathcal{R}_4\}$, $\mathcal{D}_2 = \{\mathcal{R}_1, \mathcal{C}_2, \mathcal{R}_3, \mathcal{R}_4\}$, $\mathcal{D}_3 = \{\mathcal{R}_1, \mathcal{C}_2, \mathcal{C}_3, \mathcal{R}_4\}$, $\mathcal{D}_4 = \{\mathcal{R}_1, \mathcal{C}_2, \mathcal{C}_3, \mathcal{C}_4\}$ and $\mathcal{D}_5 = \{\mathcal{C}_1, \mathcal{C}_2, \mathcal{C}_3, \mathcal{C}_4\}$

5.1 MNIST Datasets

We modified the MNIST dataset [9] to simulate temporal and longitudinal effects. To simulate heterogeneity and the effect of different observation likelihoods, we divided each image into 4 regions, $\mathcal{R}_1, \dots, \mathcal{R}_4$ and created five different datasets, $\mathcal{D}_1, \dots, \mathcal{D}_5$, as shown in Fig. 2. Additionally, we masked 25% of the pixels during the training and performed 5 independent runs with each dataset.

Temporal setting: A digit is manipulated by a rotation around the centre, a diagonal shift, and a change in the intensity correlated through a time covariate. The manipulated MNIST images correspond to Y in the dataset and the rotation, shift, intensity, and time correspond to the X values [20]. We compared L-VAE and HL-VAE in unseen digit prediction based on rotation, shift, intensity, and time covariates. The experiment results are shown in Fig. 3. HL-VAE outperforms L-VAE in terms of negative log-likelihood (NLL) and prediction error. The accuracy for L-VAE was obtained by discretisation of the predicted continuous values.

Longitudinal setting: We modified the simulated Health MNIST data used in [19]. The dataset aims to mimic medical data, where subjects (i.e., MNIST digits) with disease rotate in a sequence of 20 rotations depending on the time to disease diagnosis. Age-related effects are applied by shifting the digits towards the right corner over time. We evaluated the models in terms of two prediction tasks for longitudinal MNIST datasets. Firstly, we compared L-VAE and HL-VAE in terms of longitudinal data prediction; we evaluated the performance of predicting

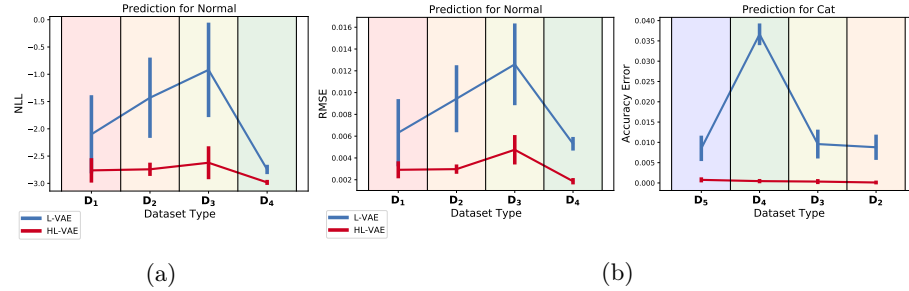


Fig. 3: Comparison of unseen test digit prediction from auxiliary covariates of HL-VAE and L-VAE (lower is better) for temporal MNIST datasets in terms of (a) NLL for real-valued sections of the digits of $\mathcal{D}_1, \dots, \mathcal{D}_4$ and (b) RMSE for real values (for $\mathcal{D}_1, \dots, \mathcal{D}_4$) and accuracy error for categorical values (for $\mathcal{D}_5, \dots, \mathcal{D}_2$). The datasets are ordered in descending order of number of variables for corresponding variable type. Vertical bars correspond to standard deviation across 5 runs.

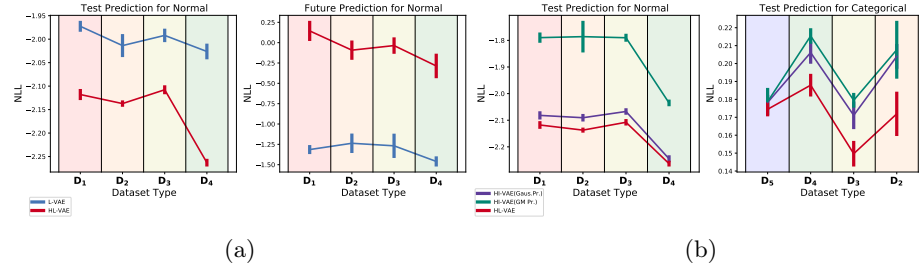


Fig. 4: Comparison of HL-VAE with other models for longitudinal MNIST datasets in terms of NLL (lower is better). a) Missing value prediction in test datasets and prediction of unseen future visits for L-VAE and HL-VAE with datasets $\mathcal{D}_1, \dots, \mathcal{D}_4$ for the real-valued data (regions). b) Missing value prediction in test datasets for HI-VAE (with Gaussian and GM prior) and HL-VAE for categorical ($\mathcal{D}_5, \dots, \mathcal{D}_2$) (left) and real-valued data ($\mathcal{D}_1, \dots, \mathcal{D}_4$) (right).

completely unobserved future time points given some new covariate information. Secondly, we compared two variations of HI-VAE, namely Gaussian prior HI-VAE and Gaussian mixture (GM) prior HI-VAE, and HL-VAE. Moreover, we also compared L-VAE and HL-VAE in terms of missing value prediction in the test split. We predicted the missing values from the observed measurements.

In order to compare L-VAE with HL-VAE, we used the same additive components in both models, namely $f_{ca}(\text{id}) + f_{se}(\text{age}) + f_{ca \times se}(\text{id} \times \text{age}) + f_{ca \times se}(\text{sex} \times \text{age}) + f_{ca \times se}(\text{diseasePresence} \times \text{diseaseAge})$. Also, we make use of the same definition for diseasePresence and diseaseAge as [19]. The comparison of these two methods in terms of error is given in Table 2 and comparison in terms of pre-

Table 2: Errors for future prediction and predicting missing values in longitudinal MNIST test splits for L-VAE and HL-VAE (lower is better). (a) Categorical (accuracy error by discretisation of continuous predictions) and (b) real-valued variables (RMSE)

Categorical			Normal		
Dataset	L-VAE ↓	HL-VAE ↓	Dataset	L-VAE ↓	HL-VAE ↓
Future Prediction					
<i>D</i> ₂ (1Q Cat)					
<i>D</i> ₂ (1Q Cat)	0.109 ± 0.005	0.084 ± 0.001	<i>D</i> ₁ (Real)	0.045 ± 0.002	0.049 ± 0.001
<i>D</i> ₃ (2Q Cat)	0.097 ± 0.005	0.076 ± 0.002	<i>D</i> ₂ (1Q Cat)	0.046 ± 0.001	0.049 ± 0.001
<i>D</i> ₄ (3Q Cat)	0.121 ± 0.008	0.097 ± 0.002	<i>D</i> ₃ (2Q Cat)	0.050 ± 0.005	0.055 ± 0.002
<i>D</i> ₅ (All Cat)	0.109 ± 0.008	0.088 ± 0.001	<i>D</i> ₄ (3Q Cat)	0.032 ± 0.004	0.038 ± 0.001
Test Prediction					
<i>D</i> ₂ (1Q Cat)	0.092 ± 0.008	0.059 ± 0.004	<i>D</i> ₁ (Real)	0.033 ± 0.002	0.021 ± 0.001
<i>D</i> ₃ (2Q Cat)	0.084 ± 0.005	0.052 ± 0.004	<i>D</i> ₂ (1Q Cat)	0.032 ± 0.002	0.021 ± 0.001
<i>D</i> ₄ (3Q Cat)	0.101 ± 0.011	0.066 ± 0.003	<i>D</i> ₃ (2Q Cat)	0.035 ± 0.003	0.022 ± 0.001
<i>D</i> ₅ (Cat)	0.093 ± 0.009	0.061 ± 0.002	<i>D</i> ₄ (3Q Cat)	0.023 ± 0.003	0.014 ± 0.001

(a) Accuracy Error

(b) RMSE

dictive NLL is given in Fig. 4a. HL-VAE outperforms L-VAE in all cases except the predictive NLL and error for the normally distributed variables of the future predictions.

Since HI-VAE cannot handle longitudinal data, we only compared against it for missing value prediction. As shown in Fig. 4b, HL-VAE outperforms both variations of HI-VAE in all cases. HL-VAE also has a better performance in terms of RMSE; detailed comparison can be found in Supp. Fig. 11.

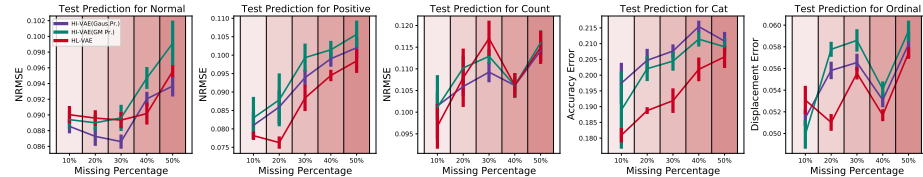


Fig. 5: Comparison of the missing value prediction errors in test splits (lower is better) for HI-VAE with Gaussian prior, HI-VAE with Gaussian mixture prior, and HL-VAE on PPMI dataset with various missing ratios, ranging from 10% to 50% for all of the five likelihoods.

5.2 A dataset from the PPMI

This dataset (PPMI) is obtained from a large-scale, open access, international database containing multiple Parkinson’s disease (PD) cohorts with longitudinal multimodal observational studies [12]. We used a curated dataset from the

Table 3: Comparison in terms of predictive (a) NLL and (b) NRMSE for missing time point prediction and predicting missing values in PPMI test splits for L-VAE and HL-VAE (lower is better).

Normal			Non Categorical		
Dataset	L-VAE ↓	HL-VAE ↓	Dataset	L-VAE ↓	HL-VAE ↓
Future Prediction					
10% Missing	3.01 ± 0.36	3.25 ± 0.11	10% Missing	0.099 ± 0.003	0.086 ± 0.002
20% Missing	2.90 ± 0.24	3.13 ± 0.13	20% Missing	0.097 ± 0.001	0.086 ± 0.003
30% Missing	3.42 ± 0.69	2.99 ± 0.03	30% Missing	0.1 ± 0.001	0.091 ± 0.002
40% Missing	4.80 ± 0.98	3.15 ± 0.05	40% Missing	0.102 ± 0.001	0.088 ± 0.004
50% Missing	6.26 ± 0.57	3.18 ± 0.09	50% Missing	0.105 ± 0.002	0.094 ± 0.002
Test Prediction					
10% Missing	3.44 ± 0.79	3.21 ± 0.14	10% Missing	0.093 ± 0.004	0.079 ± 0.003
20% Missing	3.22 ± 0.49	3.06 ± 0.04	20% Missing	0.091 ± 0.002	0.080 ± 0.003
30% Missing	3.59 ± 0.89	3.40 ± 0.03	30% Missing	0.094 ± 0.002	0.087 ± 0.003
40% Missing	4.91 ± 1.11	3.10 ± 0.05	40% Missing	0.095 ± 0.001	0.085 ± 0.001
50% Missing	6.24 ± 0.76	3.29 ± 0.10	50% Missing	0.099 ± 0.001	0.091 ± 0.003

(a) NLL

(b) NRMSE

database that consists of demographic information, motor/non-motor assessments, cognitive tests, DaTSCAN, cerebrospinal fluid results, and biospecimen as well as genetics information. In total we had 80 heterogeneous metrics which can be modelled as 8 Gaussian, 12 log-normal, 12 Poisson, 12 ordinal logit with various levels, and 36 categorical logit model with various numbers of categories. In addition to measurements, we used the information about the participants and their visits, such as id, gender, age at visit, and participant group as covariate information. The dataset consists of 545 participants (174 healthy and 371 in the PD group) who were monitored for 5 years (i.e., samples were taken annually from the first visit/baseline to the 5th year of the study; in total 3114 measurements). We randomly divided the data into training, test, and validation splits and we generated 5 different datasets by removing 10% to 50% of the data completely at random in all the splits. The PPMI data and the data preprocessing steps can be found in Supp. Section D.

We also evaluated the models for the PPMI dataset in terms of two prediction tasks with five independent runs each. We made two random visit measurements of each participant in the test split known to the model as a part of the training split to predict the remaining (unseen) visits. The performance is evaluated on the known (or artificial) missing values that we introduced. We used the normalised root mean squared error (NRMSE) for numerical values, accuracy error for categorical values, and displacement error for ordinal values, as in [15].

Since L-VAE cannot handle categorical information, we included only 44 non-categorical measurements while training the model. On the other hand, we used all the measurements for the training of HL-VAE, thereby making use of all available information. However, the comparison of the two models is per-

formed only on the 44 non-categorical measurements. The predictive NLL and error comparisons are listed in Table 3. HL-VAE performs better in almost all predictive tasks. The ability to include the categorical measurements increased the performance of the numerical measurement predictions. Additionally, as the missing percentage increases, the predicted log-likelihoods decreases for L-VAE while for HL-VAE the decrease is considerably smaller.

The comparison of HI-VAE and HL-VAE in terms of predictive error is shown in Fig. 5. In terms of predicting the missing values in the test split, HL-VAE has lower errors for all data types except for count values. The (negative) log-likelihood comparisons can be found in Supp. Figures 12 and 13.

6 Discussion

Longitudinal datasets, such as clinical trial data, contain vital information that is important to appropriately model while taking into account the intricacies such data introduces. In this paper, we proposed an extension to the VAE that can analyse high-dimensional, heterogeneous temporal and longitudinal data. Moreover, we empirically showed that our model is adept at imputing missing values as well as performing future predictions that outperform competing approaches. We demonstrated the benefits of choosing appropriate likelihood models for the data while taking the temporal aspect of the data into account. Since our model makes more appropriate assumptions about the data, we believe our work would be an important contribution to the analysis of temporal and longitudinal datasets.

Our model suffers from the same ethical concerns as most deep generative models and poses no additional risks. The authors hope that their work will only be used for applications whose ethical concerns have already been addressed.

References

1. Antelmi, L., Ayache, N., Robert, P., Lorenzi, M.: Sparse multi-channel variational autoencoder for the joint analysis of heterogeneous data. In: International Conference on Machine Learning. pp. 302–311. PMLR (2019)
2. Casale, F.P., Dalca, A.V., Saglietti, L., Listgarten, J., Fusi, N.: Gaussian process prior variational autoencoders. arXiv preprint arXiv:1810.11738 (2018)
3. Fortuin, V., Baranchuk, D., Rätsch, G., Mandt, S.: Gp-vae: Deep probabilistic time series imputation. In: International conference on artificial intelligence and statistics. pp. 1651–1661. PMLR (2020)
4. Fortuin, V., Baranchuk, D., Rätsch, G., Mandt, S.: GP-VAE: deep probabilistic time series imputation. In: The 23rd International Conference on Artificial Intelligence and Statistics, AISTATS. PMLR (2020)
5. Gootjes-Dreesbach, L., Sood, M., Sahay, A., Hofmann-Apitius, M., Fröhlich, H.: Variational autoencoder modular bayesian networks for simulation of heterogeneous clinical study data. *Frontiers in big Data* **3**, 16 (2020)
6. Hawkins-Hooker, A., Depardieu, F., Baur, S., Couairon, G., Chen, A., Bikard, D.: Generating functional protein variants with variational autoencoders. *PLoS computational biology* **17**(2), e1008736 (2021)

7. Kingma, D.P., Welling, M.: Auto-encoding variational bayes. arXiv preprint arXiv:1312.6114 (2013)
8. Lawrence, N.: Probabilistic non-linear principal component analysis with gaussian process latent variable models. *Journal of Machine Learning research* **6**(11) (2005)
9. LeCun, Y., Bottou, L., Bengio, Y., Haffner, P.: Gradient-based learning applied to document recognition. *Proceedings of the IEEE* **86**(11), 2278–2324 (1998)
10. Lopez, R., Regier, J., Cole, M.B., Jordan, M.I., Yosef, N.: Deep generative modeling for single-cell transcriptomics. *Nature methods* **15**(12), 1053–1058 (2018)
11. Ma, C., Tschiatschek, S., Turner, R., Hernández-Lobato, J.M., Zhang, C.: Vaem: a deep generative model for heterogeneous mixed type data. *Advances in Neural Information Processing Systems* **33**, 11237–11247 (2020)
12. Marek, K., Jennings, D., Lasch, S., Siderowf, A., Tanner, C., Simuni, T., Coffey, C., Kieburz, K., Flagg, E., Chowdhury, S., et al.: The parkinson progression marker initiative (ppmi). *Progress in neurobiology* **95**(4), 629–635 (2011)
13. Märtnes, K., Campbell, K., Yau, C.: Decomposing feature-level variation with covariate gaussian process latent variable models. In: *International Conference on Machine Learning*. pp. 4372–4381. PMLR (2019)
14. Moreno-Muñoz, P., Artés-Rodríguez, A., Álvarez, M.A.: Heterogeneous multi-output gaussian process prediction. arXiv preprint arXiv:1805.07633 (2018)
15. Nazabal, A., Olmos, P.M., Ghahramani, Z., Valera, I.: Handling incomplete heterogeneous data using VAEs. *Pattern Recognition* **107**, 107501 (2020)
16. Oh, M., Zhang, L.: Deepmicro: deep representation learning for disease prediction based on microbiome data. *Scientific reports* **10**(1), 1–9 (2020)
17. Polykovskiy, D., Vetrov, D.: Deterministic decoding for discrete data in variational autoencoders. In: *International Conference on Artificial Intelligence and Statistics*. pp. 3046–3056. PMLR (2020)
18. Ramchandran, S., Koskinen, M., Lähdesmäki, H.: Latent gaussian process with composite likelihoods and numerical quadrature. In: *International Conference on Artificial Intelligence and Statistics*. pp. 3718–3726. PMLR (2021)
19. Ramchandran, S., Tikhonov, G., Kujanpää, K., Koskinen, M., Lähdesmäki, H.: Longitudinal variational autoencoder. In: *International Conference on Artificial Intelligence and Statistics*. pp. 3898–3906. PMLR (2021)
20. Ramchandran, S., Tikhonov, G., Lönnroth, O., Tiikkainen, P., Lähdesmäki, H.: Learning conditional variational autoencoders with missing covariates. arXiv preprint arXiv:2203.01218 (2022)
21. Rasmussen, C.E.: Gaussian Processes in Machine Learning. In: *Advanced Lectures on Machine Learning*, pp. 63–71. Springer (2004)
22. Rasmussen, C.E., Williams, C.K.: Gaussian processes for machine learning, vol. 2. MIT press Cambridge, MA (2006)
23. Rezende, D.J., Mohamed, S., Wierstra, D.: Stochastic backpropagation and approximate inference in deep generative models. In: *Proceedings of the 31th International Conference on Machine Learning, ICML* (2014)
24. Roberts, S., Osborne, M., Ebden, M., Reece, S., Gibson, N., Aigrain, S.: Gaussian processes for time-series modelling. *Philosophical Transactions of the Royal Society A: Mathematical, Physical and Engineering Sciences* **371**(1984), 20110550 (2013)
25. Valera, I., Pradier, M.F., Ghahramani, Z.: General latent feature modeling for data exploration tasks. arXiv preprint arXiv:1707.08352 (2017)
26. Zhao, H., Rai, P., Du, L., Buntine, W., Phung, D., Zhou, M.: Variational autoencoders for sparse and overdispersed discrete data. In: *International Conference on Artificial Intelligence and Statistics*. pp. 1684–1694. PMLR (2020)

A Error metrics

We compare the models for the longitudinal MNIST dataset in terms of root mean square error (RMSE) (Eq. 11) for normally distributed values because the pixel values are transformed within the interval [0,1]. We use accuracy error (Eq. 12) for the calculation of the categorical values.

$$e_{\text{normal}} = \sqrt{\frac{1}{n} \sum_n (y_{nd} - \hat{y}_{nd})^2} \quad (11)$$

$$e_{\text{cat}} = \frac{1}{n} \sum_n \mathbb{I}(y_{nd} \neq \hat{y}_{nd}) \quad (12)$$

We simulate the longitudinal MNIST dataset for categorical values using equal-frequency discretisation as shown in Fig. 6. We use the corresponding values as categorical values for the HL-VAE, and we treat the discretised values as continuous values for the L-VAE. After prediction using L-VAE, the predicted values are discretised again, and we calculate the accuracy errors accordingly.

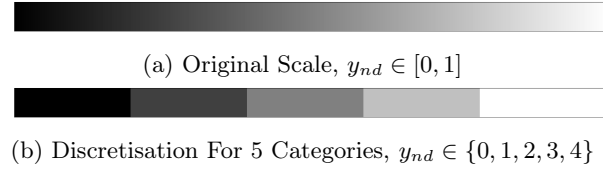


Fig. 6: Equal-Frequency Discretisation of MNIST For Categorical Values

We use the same error metrics as described in [15] for the PPMI dataset. We use the normalised root mean squared error (Eq. 13) for Gaussian, log-normal, Poisson, and beta distributed variables. Moreover, for categorical values we make use of the accuracy error (Eq. 14), and for ordinal values we make use of the displacement error (Eq. 15).

$$e_{\text{numerical}} = \frac{\sqrt{\frac{1}{n} \sum_n (y_{nd} - \hat{y}_{nd})^2}}{\max(\mathbf{y}_d) - \min(\mathbf{y}_d)} \quad (13)$$

$$e_{\text{cat}} = \frac{1}{n} \sum_n \mathbb{I}(y_{nd} \neq \hat{y}_{nd}) \quad (14)$$

$$e_{\text{ordinal}} = \frac{1}{n} \sum_n \frac{|y_{nd} - \hat{y}_{nd}|}{R} \quad (15)$$

To get the overall error metric, we take the mean of the errors for each data type as given in Eq. 16,

$$E_{\text{type}} = \frac{1}{|D_{\text{type}}|} \sum_{d_{\text{type}}} e_{\text{type}} \quad (16)$$

where ‘type’ can take any of the values in {normal, positive, count, beta, cat, ordinal}.

B Model configurations

L-VAE mainly differs from the other models on the inference network’s input dimensions and the observation model of the generative network structure.

Table 4 and Table 5 describe the inference and the generative network structures, respectively, for the longitudinal MNIST experiments. The network structure for L-VAE is the same as in [19]. The network structures differ for the input and the last layer of the generative network. In Table 4,

$$\begin{aligned} M_1 &= D_{\text{normal}} + 5 \times D_{\text{cat}} \\ M_2 &= D_{\text{normal}} + 5 \times D_{\text{cat}} + s_{\text{dim}}, \end{aligned}$$

where D_{normal} and D_{cat} are the number of dimensions for normally distributed (real-valued) and categorical variables, respectively, and s_{dim} is the number of Gaussian mixtures for Gaussian mixture prior HI-VAE. Since the categorical values are represented with one-hot encoding, there are additional independent representation neural networks before the convolutional layers where the one-hot encodings are flattened into a 1 dimensional tensor with a linear transformation layer. Another modification for the longitudinal MNIST dataset with heterogeneous modelling is that there are U *out-channels* at the last transposed convolutional layer, where U is the hyperparameter which indicates the number of input dimensions of $h_d(\cdot)$. In our experiments, we set $U = 5$. In Table 5, the number of output dimensions is calculated as follows:

$$G = \sum_{d=1}^D W_d = 2 \times D_{\text{normal}} + 4 \times D_{\text{cat}},$$

which indicates the number of likelihood parameters for HI-VAE and HL-VAE.

For the training of PPMI, a multi-layer perceptron network with a single hidden layer is used for both inference and generative networks. Table 6 lists the details of the networks. The input data for categorical and ordinal values are represented with one-hot encoding and thermometer encoding, respectively, for HI-VAE and HL-VAE. Gaussian mixture prior HI-VAE (Gaus. Pr. HI-VAE) has 5 additional dimensions because of the hyperparameter $s_{\text{dim}} = 5$. We also set U to 5 so that the dimension of the homogeneous layer is 400. Finally, the output dimensions of HI-VAE and HL-VAE correspond to the number of likelihood parameters.

Table 4: Inference network structures for Longitudinal MNIST datasets

Hyperparameter	HI-VAE (Gaus. Prior)	HI-VAE (GM Prior)	HL-VAE	L-VAE
Input dimension	M_1	M_2	M_1	36×36
Representation network	✓	✓	✓	✗
Number of convolution layers	2	2	2	2
Number of filters per convolution layer	144	144	144	144
Kernel size	3×3	3×3	3×3	3×3
Stride	2	2	2	2
Pooling	Max pooling	Max pooling	Max pooling	Max pooling
Pooling kernel size	2×2	2×2	2×2	2×2
Pooling stride	2	2	2	2
Number of feedforward layers	1	1	1	2
Width of feedforward layers	500	500	500	300,30
Dimensionality of latent space	32	32	32	32
Activation function of layers	RELU	RELU	RELU	RELU

C MNIST datasets

C.1 Temporal MNIST

To simulate a temporal dataset, we manipulated a digit from MNIST dataset in terms of rotation centred in the middle of the digit, shift along the diagonal and intensity on the pixels correlated through a time covariate as shown in Fig. 7 [20]. An example section is given in Fig. 8. The training, validation and test datasets consist of 4000, 400 and 400 observations of a digit '3'.

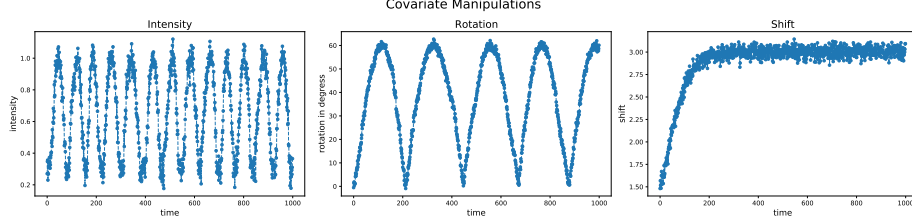


Fig. 7: Covariates of temporal MNIST dataset

C.2 Longitudinal MNIST

The whole dataset consists of 1300 subjects, where half of them are '3's and the other half are '6's. Each subject can be considered as a participant in a

Table 5: Generative network structures for Longitudinal MNIST datasets

Hyperparameter	HI-VAE (Gaus. Prior)	HI-VAE (GM Prior)	HL-VAE	L-VAE
Dimensionality of input	32	32	32	32
Number of transposed convolution layers	2	2	2	2
Number of filters for the first transposed convolution layer	256	256	256	256
Number of filters for the second transposed convolution layer	256×5	256×5	256×5	256
Kernel size	4×4	4×4	4×4	4×4
Stride	2	2	2	2
Number of fully connected layers	1	1	1	2
Width of fully connected layers	500	500	500	30,300
Activation function of layers	RELU	RELU	RELU	RELU
Number of output dimensions	G	G	G	36×36

longitudinal study, and we randomly selected half of them as healthy, and the remaining half of the subjects as developing a disease. The training split contains 1000 subjects with 20 time points, and additional 100 subjects with the first 5 time points; in total 20500 samples. The validation split contains 200 subjects with 20 time points; 4000 samples in total, and is used to avoid overfitting during training. Finally, the test split consists of the 15 remaining time point samples of the 100 subjects, whose first 5 time points are included in the training split, in total 1500 samples. Each sample has $Q = 6$ dimensional covariate information of age, id, presence of the disease (diseasePresence), age of the disease (diseaseAge), sex and location. 25% of the image data is masked during training to evaluate the models' missing value prediction performance.

D PPMI dataset

Data used in the preparation of this article was obtained from the Parkinson's Progression Markers Initiative (PPMI) database (www.ppmi-info.org/data). For up-to-date information on the study, visit www.ppmi-info.org [12].

We used the *Curated data cut-Original Cohort Baseline to Year 5 data* from the PPMI database. We eliminated the columns (i.e., features) with more than 35% actual missing values and participants with less than 4 visits. The number of categories for categorical values and the number of levels for ordinal values are listed in Table 7. The various test scores in the data that have specific values, e.g., $\{1,2,\dots,10\}$, are considered as ordinal if the number of levels is less than 10. Otherwise, we model the test score values with the Poisson distribution.

Each participant has at least four and at most six measurements/samples, and 80 heterogeneous metrics are measured (in other words, for each measurement, 80 different values are obtained). In addition to measurements, we used

Table 6: Network structures For PPMI datasets

Hyperparameter	HI-VAE (Gaus. Prior)	HI-VAE (GM Prior)	HL-VAE	L-VAE
Inference network				
Input dimension	208	213	208	44
Number of fully connected layers	1	1	1	1
Width of fully connected layers	50	50	50	30
Dimensionality of latent space	8	8	8	8
Activation function of layers	RELU	RELU	RELU	RELU
Generative network				
Input dimension	8	8	8	8
Number of fully connected layers	1	1	1	1
Width of fully connected layers	50	50	50	30
Activation function of layers	RELU	RELU	RELU	RELU
Homogeneous layer dimension	400	400	400	-
Output dimension	192	192	192	44

Table 7: Information on nominal variables in the PPMI dataset

Categorical		Ordinal	
# of Categories	# of Variables	# of Levels	# of Variables
2	22	3	1
3	6	4	2
4	2	5	6
6	3	7	1
7	1	8	1
8	2	9	1
Total	36	Total	12

the information about the participants and their visits, which are id, gender, age at visit, the number of months that passed from the diagnosis, the duration of symptomatic therapy for those who receive, and participant group, as covariate information.

The dataset has a total of 3114 measurements with 5.5% of unobserved (actual missing) values. We use 5 different missing value masks with 10%, 20%, 30%, 40%, and 50% of data assumed as missing without considering the actual missing values. We calculate the evaluation metrics for the masked values for which the actual values are known. Therefore, we calculate the evaluation metrics for 9.5 %, 19%, 28%, 38%, and 47% of the values for the corresponding datasets.

We selected 91 participants (chosen at random) and their associated 518 measurements as the unseen test split. For the training split, we selected 387 participants (chosen at random) and their associated 2212 measurements. Moreover, we included two random visits of each participant from the test split in

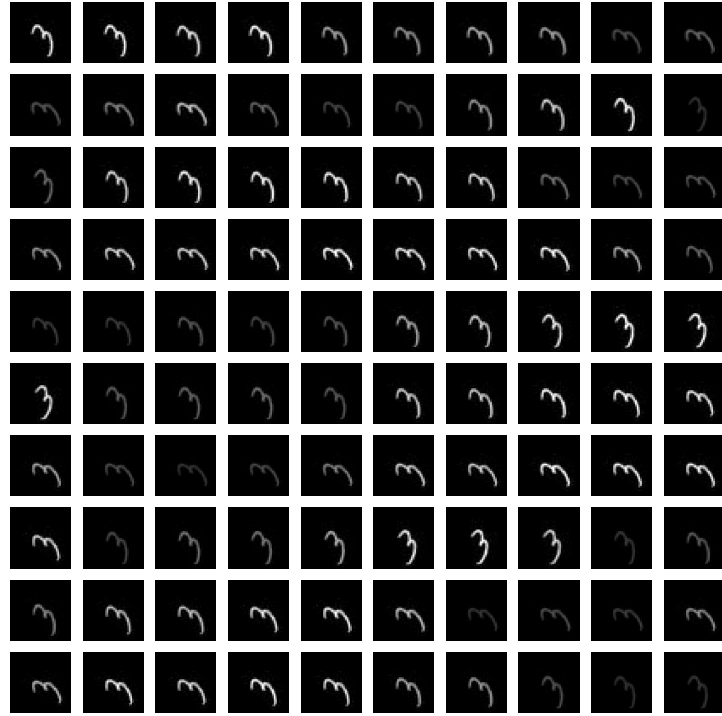


Fig. 8: Example section of temporal rotated MNIST dataset

the training dataset to facilitate the prediction of future observations. Therefore, the training set has a total of 2394 samples. Finally, we selected 67 participants at random and their associated 384 measurements as the validation split. We generated 5 different datasets by removing completely at random 10% to 50% of the data.

E Supplementary results

The additional results for the experiments are shown in Figures 9, 10, 11, 12, and 13.

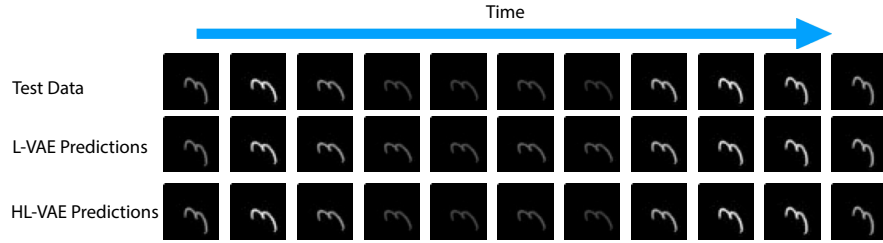


Fig. 9: An example reconstruction from temporal MNIST test data and corresponding prediction of L-VAE and HL-VAE from auxiliary covariates.

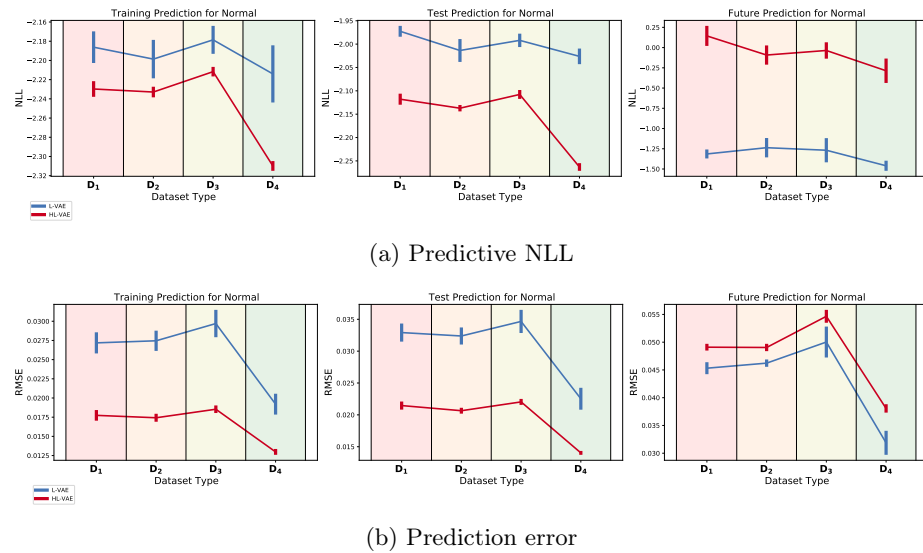


Fig. 10: Comparison of L-VAE and HL-VAE with longitudinal MNIST datasets, D_1, \dots, D_4 for real-valued variables. (a) Predictive NLLs and (b) prediction errors of the models for missing value prediction of normally distributed values in training as well as test datasets and prediction of unseen future visits.

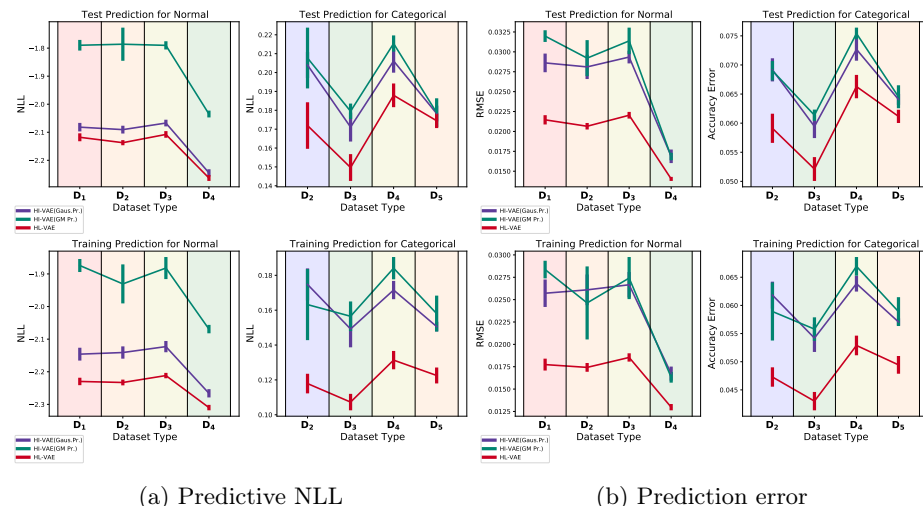


Fig. 11: Comparison of HI-VAE and HL-VAE with longitudinal MNIST datasets, $\mathcal{D}_1, \dots, \mathcal{D}_5$. (a) Predictive NLLs and (b) prediction errors of the models for missing value prediction in training and test datasets.

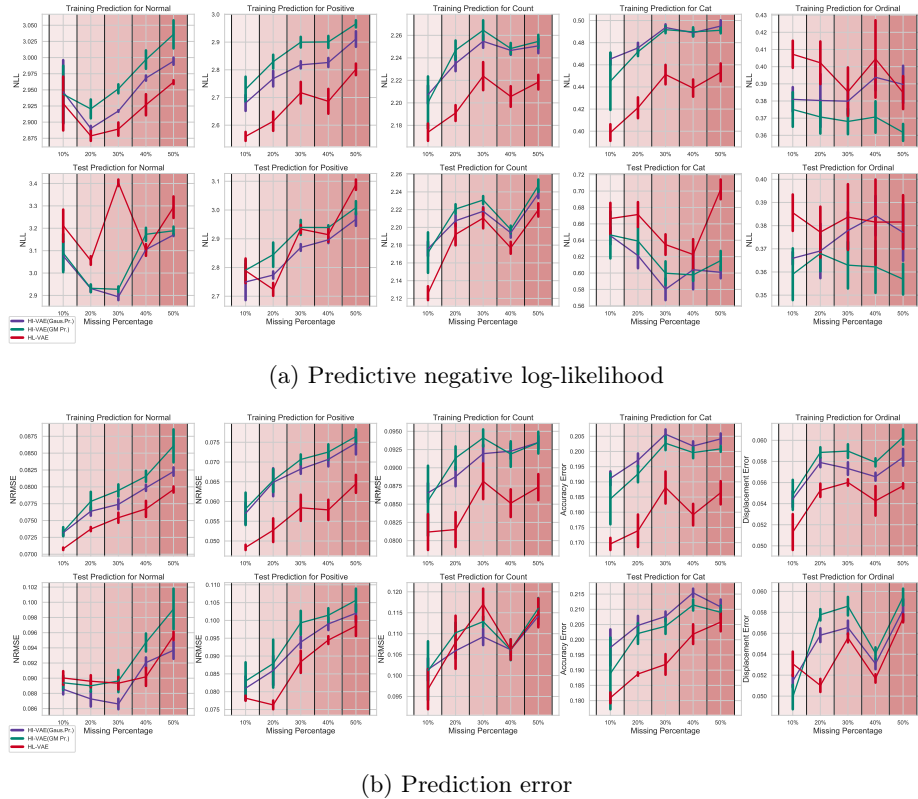


Fig. 12: Comparison of HI-VAE with Gaussian prior (Gaus. Pr.), HI-VAE with Gaussian mixture prior (GM Pr.), and HL-VAE with PPMI dataset for all of the five likelihoods. (a) Predictive negative log-likelihoods of the models for missing value prediction in training and test datasets, (b) prediction errors of the corresponding evaluation criteria.

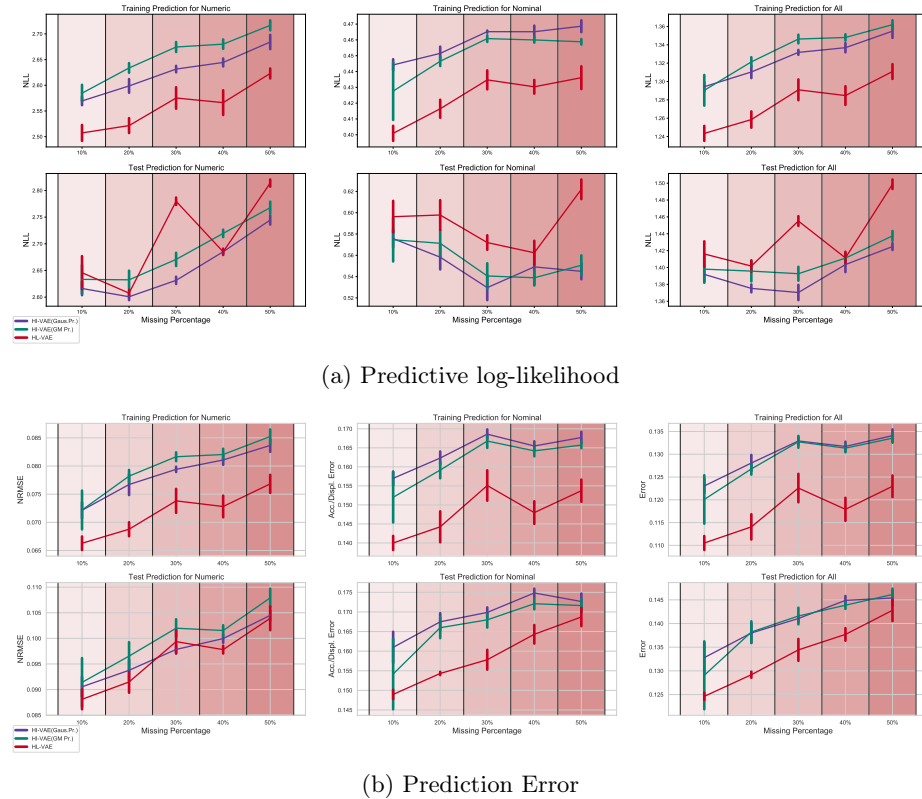


Fig. 13: Comparison of HI-VAE with Gaussian prior (Gaus. Pr.), HI-VAE with Gaussian mixture prior (GM Pr.), and HL-VAE with PPMI dataset for numeric values, nominal values, and all of the measurement values. (a) Predictive negative log-likelihoods of the models for missing value prediction in training and test datasets, (b) prediction errors of the corresponding evaluation criteria.